Research Article

Design of Wireless Nanosensor Networks for Intrabody Application

Suk Jin Lee,[1] Changyong (Andrew) Jung,[2] Kyusun Choi,[3] and Sungun Kim[4]

[1] *Texas A&M University-Texarkana, Texarkana, TX 75503, USA*
[2] *Framingham State University, Framingham, MA 01701, USA*
[3] *Pennsylvania State University, University Park, PA 16802, USA*
[4] *Pukyong National University, Busan 608-737, Republic of Korea*

Correspondence should be addressed to Sungun Kim; kimsu@pknu.ac.kr

Emerging nanotechnology presents great potential to change human society. Nanoscale devices are able to be included with Internet. This new communication paradigm, referred to as Internet of Nanothings (IoNT), demands very short-range connections among nanoscale devices. IoNT raises many challenges to realize it. Current network protocols and techniques may not be directly applied to communicate with nanosensors. Due to the very limited capability of nanodevices, the devices must have simple communication and simple medium sharing mechanism in order to collect the data effectively from nanosensors. Moreover, nanosensors may be deployed at organs of the human body, and they may produce large data. In this process, the data transmission from nanosensors to gateway should be controlled from the energy efficiency point of view. In this paper, we propose a wireless nanosensor network (WNSN) at the nanoscale that would be useful for intrabody disease detection. The proposed conceptual network model is based on On-Off Keying (OOK) protocol and TDMA framework. The model assumes hexagonal cell-based nanosensors deployed in cylindrical shape 3D hexagonal pole. We also present in this paper the analysis of the data transmission efficiency, for the various combinations of transmission methods, exploiting hybrid, direct, and multi-hop methods.

1. Introduction

Nanoscale devices require a new communication paradigm; they perform simple tasks, share the collected data, and reach unprecedented number of locations over the Internet. This new network paradigm is called IoNT [1]. In the IoNT, the new network architecture was proposed to accommodate two potential applications: interconnect nanoscale devices and interconnect offices. Our research work is focused on the intrabody communications for healthcare providers to develop the network system architecture for realizing IoNT applications. Human body is made up of almost 80 organs. Here, the nanosensors may be implanted into the organs, detecting specific symptom or virus and forwarding the sensing data to the nanorouter. The nanorouter may collect data from the nanosensors. The nanorouter then may send the collected data to the outside of the body.

The intrabody wireless communications encounter some difficulties that do not appear in regular propagation conditions because the human body has a lot of water. Firstly, in-body path loss model for homogeneous human tissues was investigated as a function of various parameters at 2.45 GHz range [2]. In addition, it is also discussed that the terahertz (THz) band can be the potential solution to operate the future electromagnetic (EM) nanosensors [3]. Moreover, the related studies reveal that the path loss in human tissues at very short distances (several millimeters) is not significant to deal well with communications among nanosensors at THz frequency range [4, 5]. Recently, the numerical analysis of EM wave propagation in the human body explains that using of EM paradigm is favorable compared with the molecular communication channel because the molecular channel attenuation is considerably higher than the situation using THz EM mechanism in terms of the path loss versus

distance [6]. On the other hand, the nanosensor, equipped with graphene-based nanopatch antennas, is envisaged to allow the implementation of nano-EM communications [3].

Nanonetworking is an emerging field, communicating among nanomachines and expanding the capability of a single nanomachine. Moreover, WNSN at the nanoscale may be useful for intrabody disease detection. For instance, nanosensors deployed in WNSN, equipped with graphene-based nanopatch antennas [3], can detect symptoms or virus by means of molecules [7] or bacteria behaviors [8]. In fact, the large surface area and the excellent electrical conductivity of graphene allow rapid electron transfer that facilitates accurate and selective detection of biomolecules. According to Kuila et al., the advancement of graphene-based biosensors allows the application of graphene for the detection of glucose, Cyt-c (Cytochrome-c), NADH (Nicotinamide Adenine Dinucleotide Hydride), Hb (Hemoglobin), cholesterol, AA (Amino Acid), UA (Uric Acid), and DA (Diamino Acid) [9].

In general, nanosensors have the very limited amount of energy in their batteries and it is not easy to replace or recharge them. When the energy harvesting systems are assumed in IoNT applications, the energy resources of nanosensors might be retained over time. That is because the nanoscale power generator could convert mechanical movement, vibrational movement, or hydraulic energy into the electrical energy [10]. However, they are not easy to implement. Therefore, the data transmission method plays an important role in the optimization of the energy consumption [11]. In addition, the data transmission is one of the important factors for realizing efficient IoNT applications due to large data produced from nanosensors [12].

For example, Pierobon et al. proposed a routing and data transmission framework to optimize the use of harvested energy with multi-hop decision algorithm [13]. In this approach, the nanorouter makes decision for a nanosensor to transmit the sensing data using direct or multi-hop transmission, based on the estimated distance between the nanorouter and the nanosensor [13]. This framework follows a typical Time Division Multiple Access (TDMA) scheduling using DownLink (DL), UpLink (UL), Multi-Hop (MH), and RandomAccess (RA). However, due to the very limited capability of nanodevices, the devices must have simple communication and simple medium sharing mechanism. For this reason, our research work is based on OOK protocol and TDMA-based framework for the efficient data collection [11, 13].

Furthermore, for the various combinations of transmission methods, we also study the analysis of the data transmission efficiency for choosing the best one adapting to the suggested network model. Here, note that we produce an energy dissipation model based on the path loss model of Jornet and Akyildiz [14, 15] and also analyze the communication from single-hop as well as multi-hop. In fact, [13] revealed that the energy aware routing framework with the combination of direct and multi-hop transmission methods can prolong the network life time.

This paper deals with the design of a WNSN at the nanoscale to be used for intrabody disease detection as an application of the IoNT. The suggested model assumes hexagonal cell-based nanosensors deployed in cylindrical shape 3D hexagonal pole. Here, a hexagonal cell model represents each cell which is the smallest living unit of organs. Note that the proposed model assumes hexagonal cell-based nanosensors because the nanopatch antennas are graphene-based in a honeycomb crystal lattice.

For designing this model, at first, we explain the network architecture for the proposed IoNT application model and describe the corresponding cylindrical body model using 3D hexagonal pole. Second, for the supposed organ of the human body, we present the derivation of the ideal number of hexagonal cells and the edge length in proportion to the needed annulus number horizontally; and then we describe a comparative analysis of the energy efficiency, in the process of data transmission, showing that the selection of the data transmission method plays an important role in the optimization of energy consumption. Such a comparative analysis is done for the various combinations of data transmission methods exploiting the hybrid, direct, and multi-hop methods.

In the following section, we explain the physical and MAC layers' concepts for our proposed WNSN model for the supposed IoNT application. Accordingly, the nanosensor deployment model and the energy consumption scheme are described in Section 3. In Section 4, we present the modelling of the various combinations of transmission methods and suggest their energy dissipation equations. Section 5 describes the conceptual design of a WNSN for intrabody application and shows simulation results and comparative analysis of the data transmission efficiency, followed by conclusion and future works in Section 6.

2. Preliminary

2.1. Physical and MAC Layer Protocol Peculiarities of Nanosensors in the Proposed WNSN Model. The nanosensors, equipped with graphene-based nanopatch antennas, are envisaged to allow the implementation of nano-EM communications [3]. EM communication waves propagating in graphene-based antenna have a lower propagation speed than those in metallic antenna. Nevertheless, Gbps channel capacity is available by radiating EM waves in THz frequency range. However, our suggested model for intrabody application does not probably need such a high channel capacity. Moreover, if we assume that each nanosensor widely dispersed in the body has just a role to catch disease symptoms anyhow, we need to have a simple OOK protocol to communicate between nanorouter and each nanosensor. Here, OOK protocol can use femtosecond pulse-based modulations in which the transmitted pulse lies in THz, called IR-UWB, Impulse Radio Ultra Wide Band [11, 16]. For example, the symbol "1" is sent by using a one hundred-femtosecond-long pulse as detection of disease symptom and the symbol "0" as nondetection of disease symptom; that is, the nanosensor remains silent. In this process, we adopt a scheduling scheme based on TDMA for the synchronization among nanosensors and nanorouter. In fact, employing this scheme may lead us to need simple MAC protocol to avoid collisions in simultaneous transmissions. More details about the behavior of physical and data link layer protocols are out of the scope of this paper.
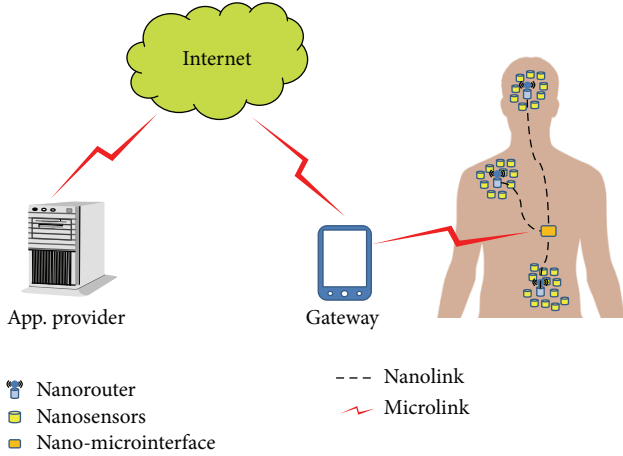
FIGURE 1: Network architecture for the proposed IoNT application model.

Anyway, Jornet et al. showed that time spread OOK protocol generates a very short pulse in femtosecond long [17], which has its main frequency components in the THz band. And that is already being used in several applications such as nanoscale spectroscopy and biological imaging [18].

2.2. Network Architecture for IoNT Applications. Figure 1 depicts simple network architecture of WNSN to be used for intrabody disease detection as an application of the IoNT [1]. The network can be composed of nanosensors, nanorouters, nano-microinterface and gateway regardless of any specific application. Here nanosensor is implanted into the organs detecting symptoms or virus, performing computation with a limited memory and transmitting small data over a short range, whereas nanorouters are relatively larger computational resources than nanosensors. They aggregate data from nanomachines (nanosensors). After nanosensors detect specific symptoms or virus, simple data (e.g., 1 for detection or 0 for nondetection) to inform the existence of symptoms or virus will be forwarded to the nano-microinterface through nanorouters. Here, the gateway (i.e., microscale device) makes it possible to remotely control the entire system over the Internet.

In this paper, we assume that the nanosensors are able to detect specific symptoms or virus by means of signal molecules [7] or bacteria behaviors [8]. Each cell in this case is modeled as a hexagonal shaped cell, therefore giving a 3D structure for the nanosensor networks. Actually the hexagonal shaped cell model is a very similar structure with the graphene in a honeycomb crystal lattice. Here, the accumulated unit layers (where the unit layer consists of unit cells) construct a 3-dimensional space for the individual target organ, for example, heart, lungs, and kidney.

3. Nanosensor Deployment and Energy Consumption Models for the Nanonetworks

3.1. Wireless Nanosensor Network Model. The nanosensors can be deployed arbitrarily at organs of the human body and they may be moved by body fluid. We assume that the nanosensors are distributed in 3-dimensional space in the nanonetworks according to a homogeneous spatial Poisson process. Most of the human organs such as spleen, liver, lung, and heart are not shaped as perpendicular structure; rather they are closer to round shape. Geometrically, we represent the organ specific targeting area of the human body as cylindrical shape 3D hexagonal pole, which is closer to the shape of organs. Here, each hexagonal shaped cell represents each cell which is the smallest living unit of organs. Thus, in the cylindrical model, as given in Figure 2, we can put as many nanosensors as possible and each hexagonal cell has one active nanosensor. Notice that the customized modeling is out of scope in this paper.

Let us define the nanonetwork depth (H) as the height of the 3D hexagonal pole. Nanosensors within each layer construct a cluster, where the information sensed by each nanosensor is transmitted to the nano-microinterface through the nanorouter of each cluster. After each nanosensor sent out the broadcasting message in a hexagonal cell, we assume that all the nanosensors may recognize other neighboring nanosensors. Each hexagonal cell may have more than one nanosensor. However, only one nanosensor that has stronger energy than others may be selected as the active nanosensor. The other nanosensors that were not selected as the active nanosensor will fall into the sleep mode, referred to as sleep nanosensors. Those sleeping nanosensors are used for the next data transmission process so that the load of the energy consumption can be evenly distributed in nanonetworks.

For the target organ, as shown in Figure 2, the edge length of hexagon S is derived from the network radius R. Once we choose the network radius R that may be relevant to the volume of the target organ, the relationship between the nanonetwork width W and the edge length of hexagon S can be visualized by the equations, as shown in Figure 2 (i.e., w is an even or odd case). Notice that the number of hexagonal cells for the individual annulus A_w is $6w$ ($w = 1, 2, \ldots, W$), where 1 is set for A_0.

Let us define ρ_i as the nanosensor density [13] of ith hexagonal cell; $\rho_i \in \{0, 1, 2, 3, \ldots\}$. After we get the relationship between the number of cells in the farthest annulus A_W and the edge length of hexagon S, we can maximize the number of each hexagonal cell X by minimizing the nanosensor density. This process allows each hexagonal cell to have a small number of nanosensors as possible. We can show this process by the following expression:

$$X = \arg\min_{X} \left[\sum_{i=1}^{3W(W+1)+1} \frac{1}{\rho_i} \right]$$
$$\text{s.t.} \quad \rho_i \neq 0, \tag{1}$$

where the hexagonal cells with no nanosensor ($\rho_i = 0$) were excluded. After choosing X, we can notice that the number of hexagonal cells that have only one nanosensor can be maximized. Our assumption is that only one nanosensor is active and the others go to sleep for the next iteration.

3.2. Energy Consumption Model for Our Wireless Nanosensor Network. Jornet and Akyildiz introduced a novel propagation model for future EM nanonetworks in the THz band.
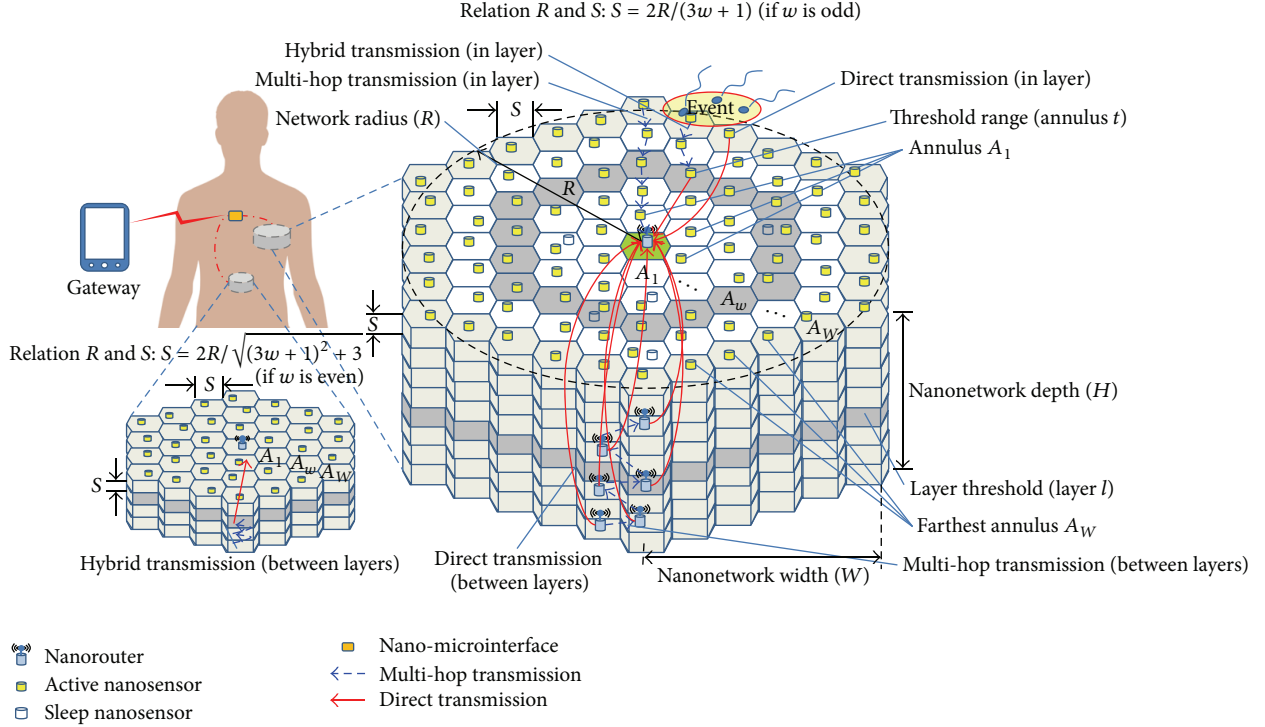
Relation R and S: $S = 2R/(3w + 1)$ (if w is odd)

Figure 2: Cylindrical shape 3D hexagonal pole.

THz path loss model of nanonetworks is obtained by using the sum in dB of the spreading loss, L_{spread}, and the molecular absorption loss, L_{abs}, as follows [14, 15]:

$$L(f,d) = L_{spread}(f,d) + L_{abs}(f,d)$$
$$= \left(\frac{4\pi d f_0}{c}\right)^2 \exp(K(f)d), \tag{2}$$

where f is the wave frequency, d is the total path length, c is the speed of light in the vacuum, f_0 is the designed center frequency, and $K(f)$ is the molecular absorption coefficient. The transmission power, $P(d)$, consumed in the transmitter nanosensor, should make sure that a constant signal-to-noise ratio (SNR) in the receiver nanosensor located at the distance d. This is defined as follows [13]:

$$P(d) = \text{SNR} \int L(f,d) N_0 df, \tag{3}$$

where N_0 is the total molecular absorption noise power spectral density. We assume that N_0 is a constant value [13]. The maximum transmission capacity of the THz band, as a function of distance d, can be calculated as follows [11]:

$$C(d) = B_{3\,dB}(d) \log_2(1 + \text{SNR}), \tag{4}$$

where $B_{3\,dB}$ is the 3 dB bandwidth. Let us define $e_t(k,d)$ as the transmitter energy dissipation to transmit k-bits packet located at the distance d. Accordingly, the transmitter energy dissipation $e_t(k,d)$ can be expressed as follows:

$$e_t(k,d) = \frac{P(d)}{C(d)} \times k = \left(\frac{4\pi d f_0}{c}\right)^2 \frac{N_0 \text{SNR}}{\log_2(1+\text{SNR})} d^2 k. \tag{5}$$

In (5), we assume that the molecular absorption does not affect the frequency range defined by the 3 dB bandwidth, $B_{3\,dB}(d)$; that is, $k(f) \approx 0$. In [16], generally, in the simple radio energy dissipation model, they introduced that the transmitter energy consumption is depending on the electronic energy and the amplifier energy, whereas the receiver energy consumption is only relevant to the electronic energy [16]. Therefore, we can define $e_r(k,d)$ as the receiver energy dissipation to receive k-bits packet and the value of $e_r(k,d)$ is intrinsically less than $e_t(k,d)$. In our model, we assume that the value of $e_r(k,d)$ is pertaining to the value of $e_t(k,d)$. Accordingly, we can derive the receiver energy dissipation (6) by substituting the constant unit distance d_0 for the transmission distance factor d as follows:

$$e_r(k,d_0) = \eta \times e_t(k,d_0), \tag{6}$$

where η is the transceiver energy dissipation ratio with the condition; that is, $\eta < 1$. For the notation simplicity, we use the receiver energy dissipation $e_r(k)$ instead of $e_r(k,d_0)$.

4. Combination of Data Transmission Methods and Energy Dissipation

4.1. Data Transmission Methods within Layer and between Layers. In this section, we introduce data transmission methods to collect the data sensed from the nanosensors. Within each layer, as shown in Figure 2, all the information detected at the nanosensors (actually we assume that this information contains the geographical location of the nanosensor that sent the symbol "1") is transmitted to the nanorouter in its

corresponding layer. Note that each nanorouter is located at the center cell (annulus A_0) of each layer and also served as an active nanosensor at the same time. On the other hand, between layers, all the collected data at the nanorouter of each layer are sent to layer 0's nanorouter that forwards the collected data to the nano-microinterface to communicate with microscale devices, that is, gateway.

First, within each layer, three data transmission methods are possible horizontally, as described in Figure 2. In the direct data transmission, every nanosensor sends the sensing data directly to its corresponding nanorouter with achieving high transmission efficiency [13]. Meanwhile, in the multi-hop transmission, an adjacent (immediate neighbor) nanosensor one annulus nearer to the corresponding nanorouter is randomly selected; and then each nanosensor which detects symptoms or virus sends the data to the chosen adjacent nanosensor until arriving at its corresponding nanorouter in the way of annulus by annulus hierarchically. On the other hand, the hybrid data transmission is achieved by combining the multi-hop and direct transmission methods. For example, let us define t as the threshold range and w as a certain annulus number in the given layer. Then, within the threshold range, t ($w \leq t$), every nanosensor sends the data directly to the nanorouter of its corresponding layer. However, for nanosensors located outside annulus t, that is, $w > t$, each one sends out the data to the adjacent (immediate neighbor) active nanosensor one annulus nearer to its nanorouter using the multi-hop transmission.

Second, between layers, three data transmission methods are also feasible as shown in Figure 2. In the hybrid approach, the collected data in each layer's router should be forwarded to the next immediate router using the multi-hop or direct transmission, where the transmission method is chosen by the threshold layer l. Let us define h as a certain layer of nanonetworks. If layer h is less than or equal to the threshold layer l; the nanorouter directly sends the collected data to layer 0's nanorouter; otherwise, the other nanorouters transmit the data to the next upper layer's nanorouter until arriving at the nanorouter of the threshold layer l using multi-hop transmission. On the other hand, the multi-hop transmission is accomplished by sending the collected data from the farthest nanorouter of layer h to the adjacent router (immediate neighbor router) until arriving at layer 0's nanorouter in the way of layer by layer hierarchically, as given in Figure 2. On the contrary, the direct data transmission can be achieved by sending the data collected at each layer's nanorouter directly to layer 0's nanorouter as explained in Figure 2.

4.2. Selection of Energy Efficient Data Transmission Method. Employing the data transmission methods within layer and between layers, explained in the previous section, we can select the most effective combination of data transmission methods in the way of energy efficiency. For the overall collection process, individual nanosensor creates a cluster for each layer, as shown in Figure 2. Each layer can select the nanorouter in its corresponding layer. Here, note that we fixed the location of each router at the center cell (annulus A_0) in each layer. After detecting symptoms or virus for the specific application, all nanosensors transmit the
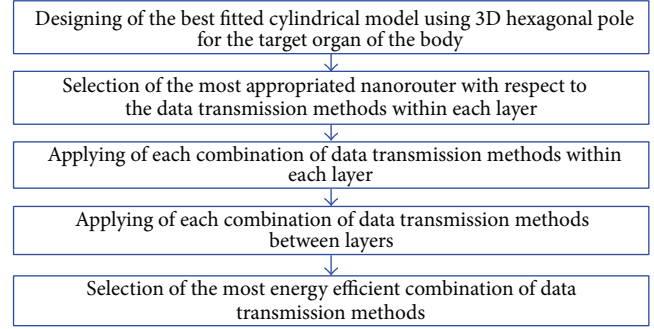

FIGURE 3: Selection of the energy efficient data transmission method.

geographical location data to their nanorouters using data transmission methods within layer, that is, hybrid method (H), multi-hop method (M), or direct method (D). After receiving the data from nanosensors, each router sends out the collected data to layer 0's router using data transmission methods between layers, that is, H, M, or D methods. Figure 3 summarizes the overall collection process.

Table 1 summarizes the possible combinations of data transmission methods. With applying one of combinations of data transmission methods listed in Table 1 to the algorithm given in Figure 3, we can find out the most energy efficient combination. We define this process denoted by

$$
\text{COMB} = \min \sum_{\text{Router}=0}^{H} \left[E_{\text{Sensor}}^{\text{Horizontal}} + E_{\text{Router}}^{\text{Horizontal}} + E_{\text{Router}}^{\text{Vertical}} \right], \tag{7}
$$

where COMB is one of combinations of data transmission methods minimizing the total energy dissipation of data transmission. E_{Router} is the total energy dissipation of the nanorouter in each layer and E_{Sensor} is the total energy dissipation of nanosensors in each layer, respectively; and H means the depth of network. Therefore, the main objective is to find out the most efficient combination of data transmission methods which has the least total energy dissipation E_{Total} (i.e., COMB) in the given cylindrical model designed for intrabody application.

4.3. Energy Dissipation of Each Combination of Data Transmission Methods. In order to calculate E_{Total} (the total energy dissipation of the nanorouter and nanosensors for each combination), we need to derive $r^{\text{Hor}}_{\text{mul}}$ (the multi-hop transmission range) and $r^{\text{Hor}}_{\text{dir}(w)}$ (the direct transmission range) within layer horizontally, as given in the equations in Figure 4(a). Respectively, between layers, we also need $r^{\text{Vert}}_{\text{mul}}$ (the multi-hop transmission range) and $r^{\text{Vert}}_{\text{dir}(h)}$ (the direct transmission range) vertically, as derived in the equations in Figure 4(b). Figure 4 shows the ranges for the multi-hop and direct transmissions utilized for each combination.

In this paper, we assume that one sensor in each cell transmits its location information in case of detecting a certain symptom or virus for the specific application. For all

TABLE 1: Possible combinations of data transmission methods.

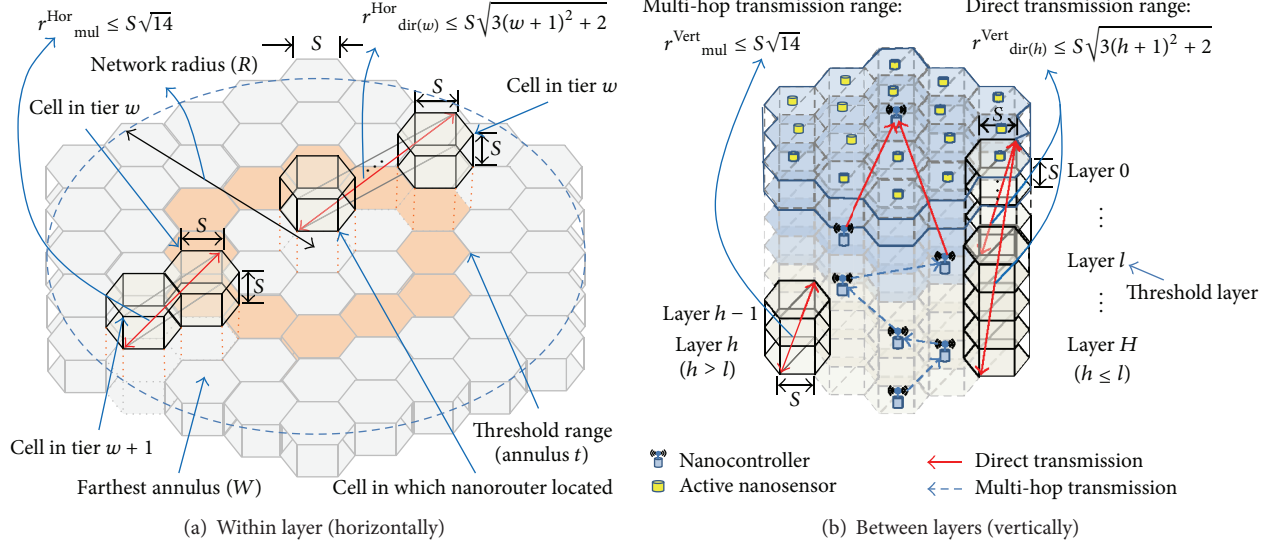| Within layer	Between layers		
	Hybrid	Multi-hop	Direct
Hybrid	Hybrid-Hybrid (H-H)	Hybrid-Multi (H-M)	Hybrid-Direct (H-D)
Multi-hop	Multi-Hybrid (M-H)	Multi-Multi (M-M)	Multi-Direct (M-D)
Direct	Direct-Hybrid (D-H)	Direct-Multi (D-M)	Direct-Direct (D-D)

FIGURE 4: Description of ranges for transmission methods.

possible combinations of data transmission methods, the energy dissipation equations are constructed as given in Table 2.

Horizontally, using (5) and (6), $r^{\text{Hor}}_{\text{mul}}$ and $r^{\text{Hor}}_{\text{dir}(w)}$ in case of applying the hybrid method in each layer, the transmission energy dissipation of nanosensors can be written as

$$E^{\text{Horizontal(Hybrid)}}_{\text{Sensor}} = 6w \times e_t\left(k, r^{\text{Hor}}_{\text{mul}}\right), \quad \text{if } w = W,$$

$$E^{\text{Horizontal(Hybrid)}}_{\text{Sensor}}$$
$$= e_r(k) \times \sum_{n=1}^{W-t-1} \left[-3n\left(n - 2W - 1\right)\right]$$
$$+ e_t\left(k, r^{\text{Hor}}_{\text{mul}}\right)$$
$$\times \sum_{n=1}^{W-t-1} \left[-3\left(n^2 + n - 2Wn - 2W\right)\right],$$
$$\text{if } t < w < W,$$

$$E^{\text{Horizontal(Hybrid)}}_{\text{Sensor}}$$
$$= e_r(k) \times \sum_{n=1}^{W-t} \left[6\left(W - n + 1\right)\right] + e_t\left(k, r^{\text{Hor}}_{\text{dir}(t)}\right)$$
$$\times \sum_{n=1}^{W-t+1} \left[6\left(W - n + 1\right)\right], \quad \text{if } w = t,$$

$$E^{\text{Horizontal(Hybrid)}}_{\text{Sensor}} = \sum_{w=1}^{t-1} \left[6w \times e_t\left(k, r^{\text{Hor}}_{\text{dir}(w)}\right)\right],$$

otherwise.

(8)

In (9), $E^{\text{Horizontal(Hybrid)}}_{\text{Sensor}}$total is the total energy dissipation of nanosensors for each layer when the hybrid transmission method is applied horizontally. Consider

$$E^{\text{Horizontal(Hybrid)}}_{\text{Sensor}}\text{total} = 6W \times e_t\left(k, r^{\text{Hor}}_{\text{mul}}\right) + e_r(k)$$
$$\times \sum_{n=1}^{W-t-1} \left[-3n\left(n - 2W - 1\right)\right] + e_t\left(k, r^{\text{Hor}}_{\text{mul}}\right)$$
$$\times \sum_{n=1}^{W-t-1} \left[-3\left(n^2 + n - 2Wn - 2W\right)\right] + e_r(k)$$
$$\times \sum_{n=1}^{W-t} \left[6\left(W - n + 1\right)\right] + e_t\left(k, r^{\text{Hor}}_{\text{dir}(t)}\right)$$
$$\times \sum_{n=1}^{W-t+1} \left[6\left(W - n + 1\right)\right]$$
$$+ \sum_{w=1}^{t-1} \left[6w \times e_t\left(k, r^{\text{Hor}}_{\text{dir}(w)}\right)\right].$$

(9)

TABLE 2: Energy dissipation of the possible combination of data transmission methods.

Methods	Total energy dissipation
H-H	$E(\text{H}, \text{H}) = E_{\text{Sensor}}^{\text{Horizontal(Hybrid)}}\text{total} + E_{\text{Router}}^{\text{Horizontal}} + E_{\text{Router}}^{\text{Vertical(Hybrid)}}\text{total} + E_{\text{Router}}^{\text{Vertical}}$
M-M	$E(\text{M}, \text{M}) = E_{\text{Sensor}}^{\text{Horizontal(Multi-hop)}}\text{total} + E_{\text{Router}}^{\text{Horizontal}} + E_{\text{Router}}^{\text{Vertical(Multi-hop)}}\text{total} + E_{\text{Router}}^{\text{Vertical}}$
D-D	$E(\text{D}, \text{D}) = E_{\text{Sensor}}^{\text{Horizontal(Direct)}}\text{total} + E_{\text{Router}}^{\text{Horizontal}} + E_{\text{Router}}^{\text{Vertical(Direct)}}\text{total} + E_{\text{Router}}^{\text{Vertical}}$
H-D	$E(\text{H}, \text{D}) = E_{\text{Sensor}}^{\text{Horizontal(Hybrid)}}\text{total} + E_{\text{Router}}^{\text{Horizontal}} + E_{\text{Router}}^{\text{Vertical(Direct)}}\text{total} + E_{\text{Router}}^{\text{Vertical}}$
H-M	$E(\text{H}, \text{M}) = E_{\text{Sensor}}^{\text{Horizontal(Hybrid)}}\text{total} + E_{\text{Router}}^{\text{Horizontal}} + E_{\text{Router}}^{\text{Vertical(Multi-hop)}}\text{total} + E_{\text{Router}}^{\text{Vertical}}$
M-H	$E(\text{M}, \text{H}) = E_{\text{Sensor}}^{\text{Horizontal(Multi-hop)}}\text{total} + E_{\text{Router}}^{\text{Horizontal}} + E_{\text{Router}}^{\text{Vertical(Hybrid)}}\text{total} + E_{\text{Router}}^{\text{Vertical}}$
M-D	$E(\text{M}, \text{D}) = E_{\text{Sensor}}^{\text{Horizontal(Multi-hop)}}\text{total} + E_{\text{Router}}^{\text{Horizontal}} + E_{\text{Router}}^{\text{Vertical(Direct)}}\text{total} + E_{\text{Router}}^{\text{Vertical}}$
D-H	$E(\text{D}, \text{H}) = E_{\text{Sensor}}^{\text{Horizontal(Direct)}}\text{total} + E_{\text{Router}}^{\text{Horizontal}} + E_{\text{Router}}^{\text{Vertical(Hybrid)}}\text{total} + E_{\text{Router}}^{\text{Vertical}}$
D-M	$E(\text{D}, \text{M}) = E_{\text{Sensor}}^{\text{Horizontal(Direct)}}\text{total} + E_{\text{Router}}^{\text{Horizontal}} + E_{\text{Router}}^{\text{Vertical(Multi-hop)}}\text{total} + E_{\text{Router}}^{\text{Vertical}}$

On the other hand, applying (5) and (6) and $r^{\text{Hor}}{}_{\text{mul}}$ in the case of the multi-hop transmission method, we derive the following equation for the transmission energy dissipation of nanosensors ($E_{\text{Sensor}}^{\text{Horizontal(Multi-hop)}}$) defined by

$$E_{\text{Sensor}}^{\text{Horizontal(Multi-hop)}} = 6w \times e_t\left(k, r^{\text{Hor}}{}_{\text{mul}}\right),$$

$$\text{if } w = W,$$

$$E_{\text{Sensor}}^{\text{Horizontal(Multi-hop)}}$$

$$= e_r(k) \times \sum_{n=1}^{W-1} [-3n(n-2W-1)] + e_t\left(k, r^{\text{Hor}}{}_{\text{mul}}\right) \quad (10)$$

$$\times \sum_{n=1}^{W-1} \left[-3\left(n^2 + n - 2Wn - 2W\right)\right],$$

$$\text{if } 0 \le w < W.$$

In (11), $E_{\text{Sensor}}^{\text{Horizontal(Multi-hop)}}\text{total}$ is the total energy dissipation of nanosensors for each layer when the multi-hop transmission method is applied horizontally. Consider

$$E_{\text{Sensor}}^{\text{Horizontal(Multi-hop)}}\text{total}$$

$$= 6W \times e_t\left(k, r^{\text{Hor}}{}_{\text{mul}}\right) + e_r(k)$$

$$\times \sum_{n=1}^{W-1} [-3n(n-2W-1)] + e_t\left(k, r^{\text{Hor}}{}_{\text{mul}}\right) \quad (11)$$

$$\times \sum_{n=1}^{W-1} \left[-3\left(n^2 + n - 2Wn - 2W\right)\right].$$

And then, applying (5) and (6) and $r^{\text{Hor}}{}_{\text{dir}(w)}$ for the direct transmission method, we can define the transmission energy dissipation of nanosensors ($E_{\text{Sensor}}^{\text{Horizontal(Direct)}}$) written as

$$E_{\text{Sensor}}^{\text{Horizontal(Direct)}}\text{total} = \sum_{w=1}^{W} \left[6w \times e_t\left(k, r^{\text{Hor}}{}_{\text{dir}(w)}\right)\right], \quad (12)$$

$$1 \le w \le W.$$

On the other hand, (13) means the total receiving energy dissipation for the nanorouter in the center cell of each layer denoted by

$$E_{\text{Router}}^{\text{Horizontal}} = (H+1) \times \left(\sum_{w=1}^{W} 6w\right) \times e_r(k), \quad (13)$$

$$0 \le l \le H.$$

Vertically, we also represent the energy dissipation of nanorouters in a similar way. First of all, using (5) and (6), $r^{\text{Vert}}{}_{\text{mul}}$, and $r^{\text{Vert}}{}_{\text{dir}(h)}$ in case of applying the hybrid transmission method, the equations for the transmission energy dissipations of nanorouters ($E_{\text{Router}}^{\text{Horizontal(Hybrid)}}$) can be written as

$$A = \left[\sum_{w=1}^{W} (6w)\right] + 1,$$

$$E_{\text{Router}}^{\text{Vertical(hybrid)}} = A \times e_t\left(k, r^{\text{Vert}}{}_{\text{mul}}\right), \quad \text{if } h = H,$$

$$E_{\text{Router}}^{\text{Vertical(hybrid)}} = e_r(k) \times \left[\sum_{n=1}^{H-l-1} (n \times A)\right]$$

$$+ e_t\left(k, r^{\text{Vert}}{}_{\text{mul}}\right)$$

$$\times \left[\sum_{n=1}^{H-l-1} [(n+1) \times A]\right],$$

$$\text{if } l < h < H,$$

$$E_{\text{Router}}^{\text{Vertical(hybrid)}} = (H-l) \times A \times e_r(k) + (H-l+1)$$

$$\times A \times e_t\left(k, r^{\text{Vert}}{}_{\text{dir}(l)}\right), \quad \text{if } h = l,$$

$$E_{\text{Router}}^{\text{Vertical(hybrid)}} = \sum_{h=1}^{l-1} \left[A \times e_t \left(k, r^{\text{Vert}}_{\text{dir}(h)} \right) \right],$$

$$\text{otherwise.} \tag{14}$$

In (15), $E_{\text{Router}}^{\text{Horizontal(Hybrid)}}$ total refers to the total energy dissipation of nanorouters when the hybrid transmission method is applied vertically. Consider

$$A = \left[\sum_{w=1}^{W} (6w) \right] + 1,$$

$$E_{\text{Router}}^{\text{Vertical(Hybrid)}} \text{ total} = A \times e_t \left(k, r^{\text{Vert}}_{\text{mul}} \right) + e_r (k)$$

$$\times \left[\sum_{n=1}^{H-l-1} (n \times A) \right]$$

$$+ e_t \left(k, r^{\text{Vert}}_{\text{mul}} \right)$$

$$\times \left[\sum_{n=1}^{H-l-1} [(n+1) \times A] \right] \tag{15}$$

$$+ (H - l) \times A \times e_r (k)$$

$$+ (H - l + 1) \times A$$

$$\times e_t \left(k, r^{\text{Vert}}_{\text{dir}(l)} \right)$$

$$+ \sum_{h=1}^{l-1} \left[A \times e_t \left(k, r^{\text{Vert}}_{\text{dir}(h)} \right) \right].$$

On the other hand, using (5) and (6) and $r^{\text{Vert}}_{\text{mul}}$ in the case of the multi-hop transmission method, we derive the transmission energy dissipation $E_{\text{Router}}^{\text{Vertical(Multi-hop)}}$ of the nanorouters given by

$$A = \left[\sum_{w=1}^{W} (6w) \right] + 1,$$

$$E_{\text{Router}}^{\text{Vertical(Multi-hop)}} = A \times e_t \left(k, r^{\text{Vert}}_{\text{mul}} \right), \quad \text{if } h = H,$$

$$E_{\text{Router}}^{\text{Vertical(Multi-hop)}} = e_r (k) \times \left[\sum_{n=1}^{H-1} (n \times A) \right]$$

$$+ e_t \left(k, r^{\text{Vert}}_{\text{mul}} \right) \tag{16}$$

$$\times \left[\sum_{n=1}^{H-1} [(n+1) \times A] \right],$$

$$\text{if } 0 \le h < H.$$

In (17), $E_{\text{Router}}^{\text{Vertical(Multi-hop)}}$ total means the total energy dissipation of nanorouters when the multi-hop transmission method is adapted vertically. Consider

$$A = \left[\sum_{w=1}^{W} (6w) \right] + 1,$$

$$E_{\text{Router}}^{\text{Vertical(Multi-hop)}} \text{ total} = A \times e_t \left(k, r^{\text{Vert}}_{\text{mul}} \right) + e_r (k)$$

$$\times \left[\sum_{n=1}^{H-1} (n \times A) \right] \tag{17}$$

$$+ e_t \left(k, r^{\text{Vert}}_{\text{mul}} \right)$$

$$\times \left[\sum_{n=1}^{H-1} [(n+1) \times A] \right].$$

And then, applying (5) and (6) and $r^{\text{Vert}}_{\text{dir}(h)}$ to the direct transmission method, (18) for the transmission energy dissipation of the nanorouters ($E_{\text{Sensor}}^{\text{Vertical(Direct)}}$) can be written as

$$A = \left[\sum_{w=1}^{W} (6w) \right] + 1,$$

$$E_{\text{Router}}^{\text{Vertical(Direct)}} \text{ total} = \sum_{h=1}^{H} \left[A \times e_t \left(k, r^{\text{Ver}}_{\text{dir}(h)} \right) \right], \tag{18}$$

$$1 \le h \le H.$$

Meanwhile, the following equation contains the total receiving energy dissipation for layer 0's nanorouter which forwards the collected information to the nano-microinterface given by

$$A = \left[\sum_{w=1}^{W} (6w) \right] + 1,$$

$$E_{\text{Router}}^{\text{Vertical}} = H \times A \times e_r (k). \tag{19}$$

Conclusively, utilizing all equations, that is, (5)-(6) and from (8) through (19), we can find the most efficient combination of data transmission methods which has the least total energy dissipation E_{Total} (i.e., COMB) in the given cylindrical model designed. According to our simulation results, we experienced that the combination of hybrid data transmissions (within layer and between layers) (H-H) outperforms other combinations like H-M, H-D, M-H, M-M, M-D, D-H, D-M, and D-D.

5. Design and Analysis of Simulation Results

5.1. Design of Nanosensors Deployment Network Model. The human body is made up of almost 80 organs; their size and weight are unpredictable according to body length, body weight, and body mass index [19]. For network modeling, we assume the target organ as cylindrical shape 3D hexagonal pole. Let us design a cylinder model for the supposed organ

TABLE 3: Number of hexagonal cells and edge length in proportion to the required annulus number.

Farthest annulus number W	10	20	30	40	50	60
Edge length of hexagon S (mm)	4.83	2.46	1.65	1.24	0.99	0.83
Total number of hexagonal cells X	331	1261	2791	4921	7651	10981

TABLE 4: Total number of layers and maximum height of network with variable edge length S.

Edge length of hexagon S (mm)	4.83	2.46	1.65	1.24	0.99	0.83
Total number of layers H	31	61	91	121	151	181
Maximum height of network (mm)	149.73	150.06	150.15	150.04	149.49	150.23

of the body (15 cm in diameter and 15 cm in height). The edge length of hexagon S can be derived by applying the relation R, as given in Figure 2. Table 3 shows S and the total number of hexagonal cells (in the layer) X in proportion to the annulus number W. In Table 3, we can notice that X increases as S decreases.

In addition, the total number of layers H can be decided by using S. Table 4 shows H and the maximum height of network approximated to 15 cm in height.

5.2. Calculation of the Horizontal Threshold Range t. For the case of the H-H combination described in Section 4.3, this section explains how to calculate the horizontal threshold range t. The total horizontal transmission energy dissipation of nanosensors is given in (9). In order to find out t for the target annulus number W in Table 3, we divide the total horizontal transmission energy dissipation ($E_{\text{Sensor}}^{\text{Horizontal(Hybrid)}}\text{total}$) by the total area ($t^2$) in the direct transmission range. For example, the horizontal energy dissipation per unit area (ΔE_{Hor}) can be calculated as follows:

$$t = \arg\min_{t} \left[\frac{E_{\text{Sensor}}^{\text{Horizontal(Hybrid)}}\text{total}}{t^2} \right]. \quad (20)$$

Figure 5 shows the energy dissipation per unit area ΔE_{Hor} versus threshold range t. In the simulation, we set the parameters as follows: the center frequency f_0 as 1 Thz, the signal-to-noise ratio (SNR) as 10 dB, the constant noise power spectral density N_0 as 3 dB, the packet size k as 256 bits, and the transceiver energy dissipation ratio η as 1/5.

As shown in Figure 5, ΔE_{Hor} has minimum value at the threshold annulus. Therefore, we can choose these threshold ranges to calculate the energy dissipation of the proposed hybrid data transmission method horizontally.

5.3. Calculation of the Vertical Threshold Layer l. This section introduces how to calculate the vertical threshold layer l, described in Section 4.3. When the hybrid data transmission method is applied between layers, (15) shows the total vertical energy consumption of nanorouters. Therefore, we need to decide threshold layer l in the way of minimizing the total

vertical energy dissipation. For this, the resulting relationship is expressed as follows:

$$l = \arg\min_{l} \left[E_{\text{Router}}^{\text{Vertical(Hybrid)}}\text{total} \right] \quad (2 \leq l < H). \quad (21)$$

Figure 6 shows the relationship between the total number of layers H and the threshold layer l. In Figure 6, we can decide the threshold layer l in the way of minimizing the energy dissipation vertically.

5.4. Energy Dissipation Analysis. For the data transmission among nanorouter and nanosensors (also among nanosensors, resp.) in each layer, three different transmission schemes, that is, H, M, and D methods, are used to compare the performance of the transceiver energy consumption. Figure 7 shows the energy dissipation of the transceivers with respect to the farthest annulus number W and the edge length S.

As shown in Figure 7, the data transmission methods, H and M, outperform the method D. In the method D, the energy consumption of the nanosensor varies with respect to the annulus number. At the initial stage (i.e., the annulus number $w = 1$), both methods, D and M, have the same energy consumption. As growing the annulus number, the energy consumption of method D is significantly increased. On the other hand, the energy consumption of method M has a constant value. In case of $w = 2$, method D consumes four times more energy than method M. Otherwise, method H has a good performance when the farthest annulus number W is more than a certain threshold, whereas method M is good overall.

On the other hand, Figure 8 compares the energy dissipation of different data transmission methods between layers, that is, method H, method M, and method D. As given in Figure 8, method H and method M show almost identical results, whereas method D consumes more energy. When the farthest annulus number W is small, the energy dissipation of method D is monotonically increased, whereas the energy dissipation is saturated when W is increased.

Figure 9 shows the energy consumption comparison of various combinations of the data transmission methods. Notice that the combinations of the direct and other methods (D-H, D-M, D-D, H-D, and M-D) destructively waste the
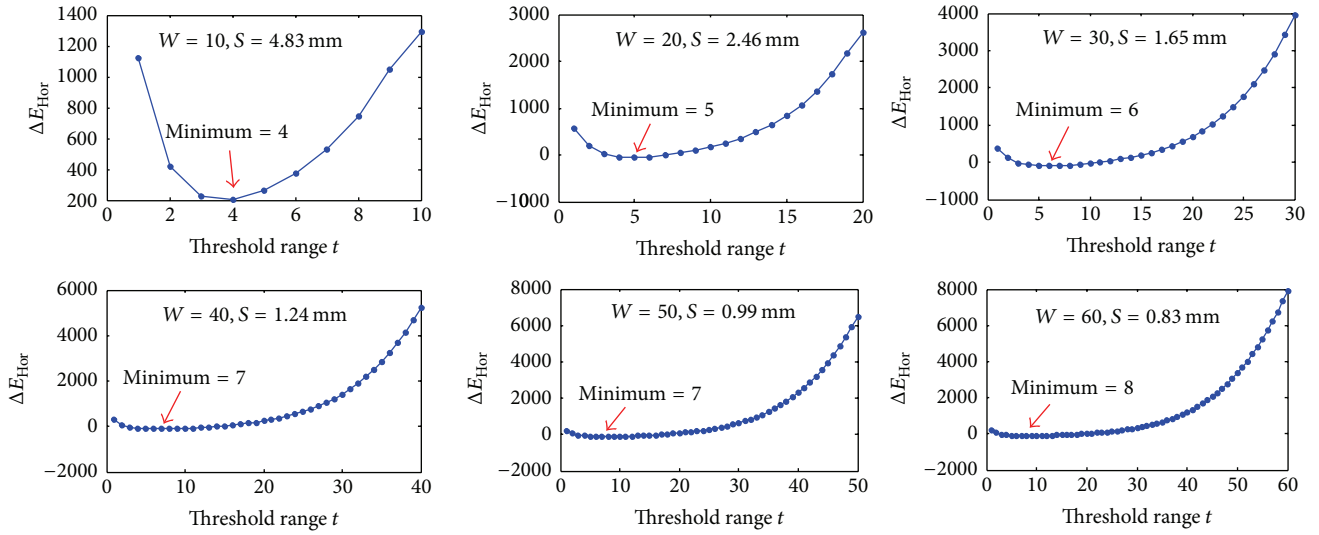
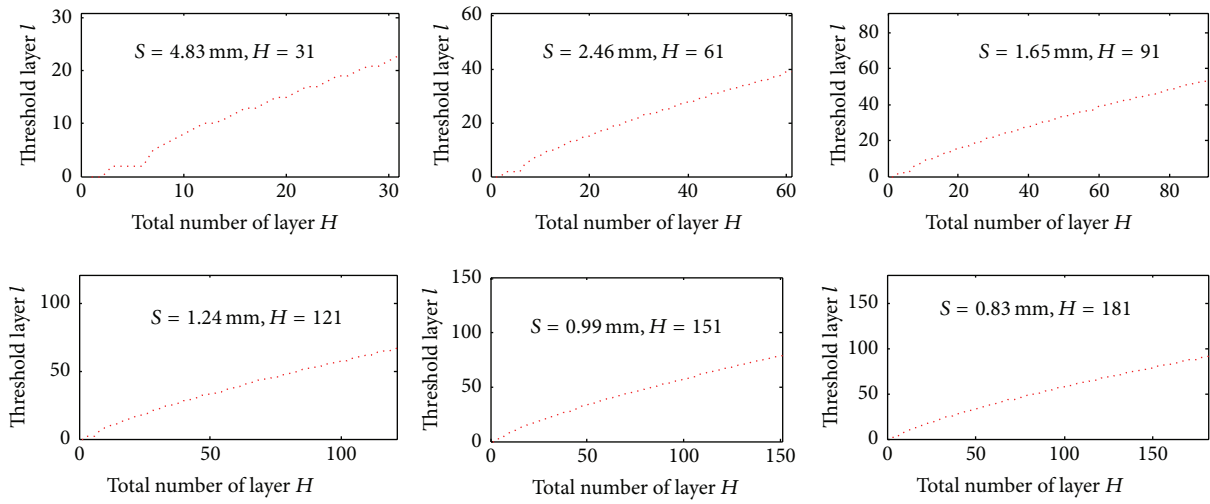FIGURE 5: Energy dissipation per unit area (ΔE_{Hor}) versus threshold range (t).

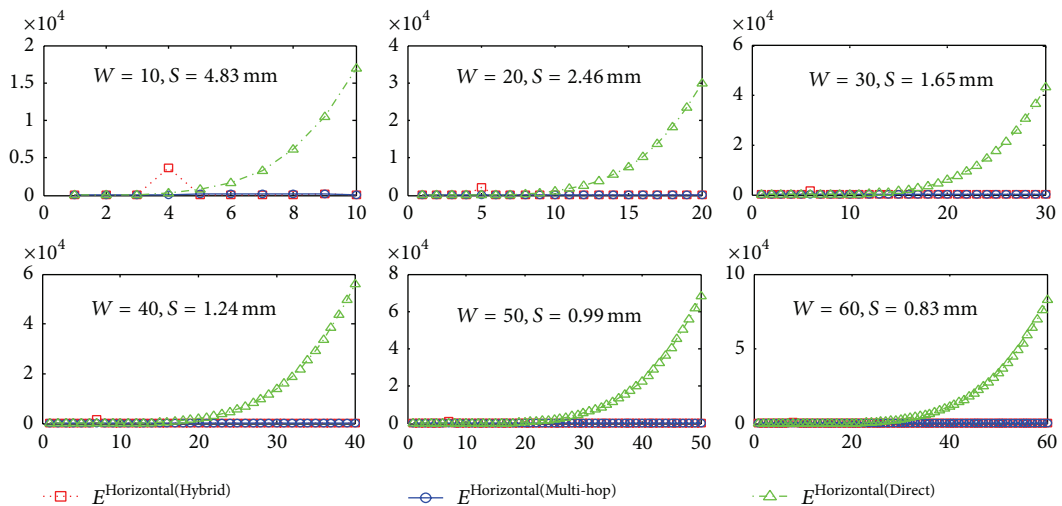FIGURE 6: Relationship between the total number of layers H and the threshold layer l.

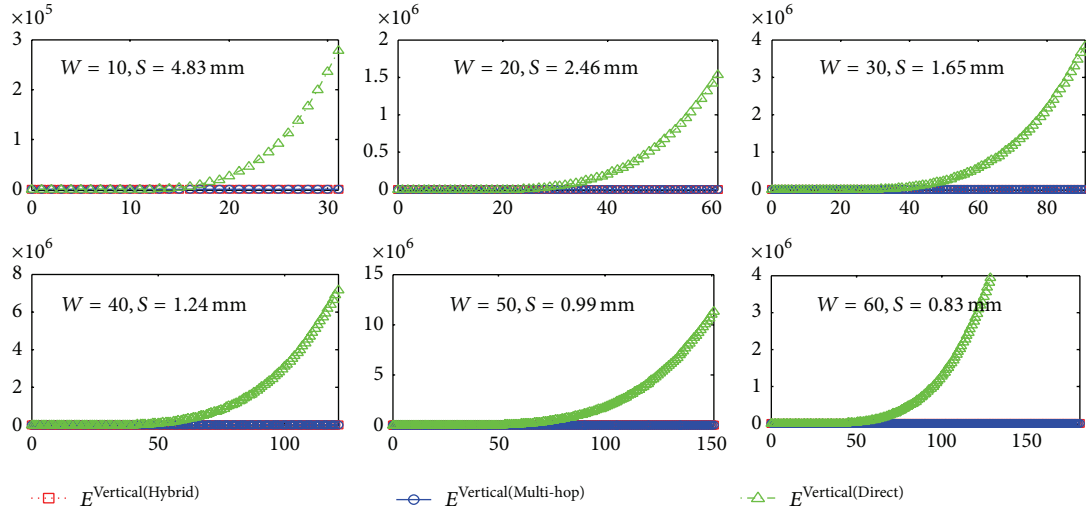FIGURE 7: Energy consumption analysis within layer.

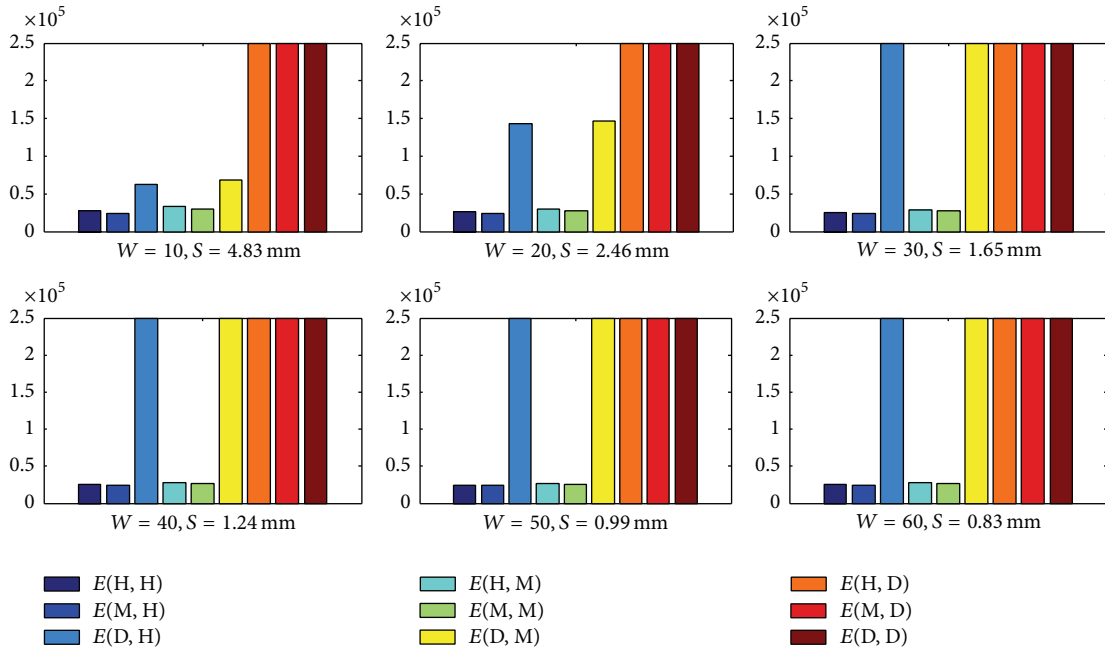FIGURE 8: Energy consumption analysis between Layers.

FIGURE 9: Energy consumption comparison of various combinations of data transmission methods.

transceiver energy compared to the combination H-H or M-H. As shown in **Figure 9**, H-H (or M-H) combination improves the average energy dissipation compared with D-H, D-M, H-D, M-D, and D-D.

6. Conclusion and Future Works

In this paper, we propose a WNSN paradigm for intrabody application. The scenario of application is that each nanosensor node would be placed within each cell and that they will communicate with their immediate neighbor cell according to the combinations of transmission methods. Each cell is

modeled as a hexagonal shaped cell, therefore giving a 3D structure for WNSN.

The contribution of this paper is twofold. First one is the derivation of the ideal number of hexagonal cells and the edge length in proportion to the needed annulus number horizontally for the supposed organ of the body. The other one is a comparative analysis of the energy efficiency in the process of data transmission, showing that H-H (or M-H) combination improves the average energy dissipation compared with D-H, D-M, H-D, M-D, and D-D combinations.

Some issues still remain to be solved in the future. First, we need to verify the proposed conceptual model in real

environment to be used for intrabody application. Second, we also need to implement the most efficient data transmission methods and the network protocols based on OOK and TDMA framework and to verify them in that environment.

Conflict of Interests

The authors declare that there is no conflict of interests regarding the publication of this paper.

Acknowledgment

References

[1] I. F. Akyildiz and J. M. Jornet, "The Internet of nano-things," *IEEE Wireless Communications*, vol. 17, no. 6, pp. 58–63, 2010.

[2] D. Kurup, W. Joseph, G. Vermeeren, and L. Martens, "In-body path loss model for homogeneous human tissues," *IEEE Transactions on Electromagnetic Compatibility*, vol. 54, no. 3, pp. 556–564, 2012.

[3] I. F. Akyildiz and J. M. Jornet, "Electromagnetic wireless nanosensor networks," *Nano Communication Networks*, vol. 1, no. 1, pp. 3–19, 2010.

[4] K. Yang, A. Alomainy, and Y. Hao, "In-vivo characterisation and numerical analysis of the THz radio channel for nanoscale body-centric wireless networks," in *Proceedings of the USNC-URSI Radio Science Meeting (Joint with AP-S Symposium) (USNC-URSI '13)*, pp. 218–219, IEEE, Lake Buena Vista, Fla, USA, July 2013.

[5] K. Yang, A. Pellegrini, A. Brizzi, A. Alomainy, and Y. Hao, "Numerical analysis of the communication channel path loss at the THz band inside the fat tissue," in *Proceedings of the IEEE MTT-S International Microwave Workshop Series on RF and Wireless Tecbhnologies for Biomedical and Healthcare Applications (IMWS-BIO '13)*, December 2013.

[6] K. Yang, A. Pellegrini, M. O. Munoz, A. Brizzi, A. Alomainy, and Y. Hao, "Numerical analysis and characterization of THz propagation channel for body-centric nano-communications," *IEEE Transactions on Terahertz Science and Technology*, vol. 5, no. 3, pp. 419–426, 2015.

[7] T. Nakano and J.-Q. Liu, "Design and analysis of molecular relay channels: an information theoretic approach," *IEEE Transactions on Nanobioscience*, vol. 9, no. 3, pp. 213–221, 2010.

[8] S. Balasubramaniam and P. Lio', "Multi-hop conjugation based bacteria nanonetworks," *IEEE Transactions on Nanobioscience*, vol. 12, no. 1, pp. 47–59, 2013.

[9] T. Kuila, S. Bose, P. Khanra, A. K. Mishra, N. H. Kim, and J. H. Lee, "Recent advances in graphene-based biosensors," *Biosensors and Bioelectronics*, vol. 26, no. 12, pp. 4637–4648, 2011.

[10] Z. L. Wang, "Energy harvesting for self-powered nanosystems," *Nano Research*, vol. 1, no. 1, pp. 1–8, 2008.

[11] P. Wang, J. M. Jornet, M. G. Abbas Malik, N. Akkari, and I. F. Akyildiz, "Energy and spectrum-aware MAC protocol for perpetual wireless nanosensor networks in the Terahertz Band," *Ad Hoc Networks*, vol. 11, no. 8, pp. 2541–2555, 2013.

[12] S. Balasubramaniam and J. Kangasharju, "Realizing the internet of nano things: challenges, solutions, and applications," *Computer*, vol. 46, no. 2, Article ID 6357163, pp. 62–68, 2013.

[13] M. Pierobon, J. M. Jornet, N. Akkari, S. Almasri, and I. F. Akyildiz, "A routing framework for energy harvesting wireless nanosensor networks in the Terahertz Band," *Wireless Networks*, vol. 20, no. 5, pp. 1169–1183, 2014.

[14] J. M. Jornet and I. F. Akyildiz, "Channel capacity of electromagnetic nanonetworks in the terahertz band," in *Proceedings of the IEEE International Conference on Communications (ICC '10)*, pp. 1–6, May 2010.

[15] J. M. Jornet and I. F. Akyildiz, "Channel modeling and capacity analysis for electromagnetic wireless nanonetworks in the terahertz band," *IEEE Transactions on Wireless Communications*, vol. 10, no. 10, pp. 3211–3221, 2011.

[16] J. M. Jornet and I. F. Akyildiz, "Information capacity of pulse-based wireless nanosensor networks," in *Proceedings of the 8th Annual IEEE Communications Society Conference on Sensor, Mesh and Ad Hoc Communications and Networks (SECON' 11)*, pp. 80–88, June 2011.

[17] J. M. Jornet, J. Capdevila Pujol, and J. Solé Pareta, "PHLAME: a physical layer aware MAC protocol for electromagnetic nanonetworks in the terahertz band," *Nano Communication Networks*, vol. 3, no. 1, pp. 74–81, 2012.

[18] D. Woolard, P. Zhao, C. Rutherglen et al., "Nanoscale imaging technology for THz-frequency transmission microscopy," *International Journal of High Speed Electronics and Systems*, vol. 18, no. 1, pp. 205–222, 2008.

[19] D. K. Molina and V. J. M. Dimaio, "Normal organ weights in men. Part II. The brain, lungs, liver, spleen, and kidneys," *The American Journal of Forensic Medicine and Pathology*, vol. 33, no. 4, pp. 368–372, 2012.